Journal of Quantitative Spectroscopy & Radiative Transfer 112 (2011) 1213–1221

Contents lists available at ScienceDirect

Journal of Quantitative Spectroscopy & Radiative Transfer

journal homepage: www.elsevier.com/locate/jqsrt

Multi-scale *k*-distribution model for gas mixtures in hypersonic nonequilibrium flows

Ankit Bansal [a], M.F. Modest [b,*], D.A. Levin [c]

[a] Department of Mechanical Engineering, The Pennsylvania State University, University Park, PA 16802, United States
[b] School of Engineering, University of California, Merced, CA 95343, United States
[c] Department of Aerospace Engineering, The Pennsylvania State University, University Park, PA 16802, United States

ARTICLE INFO

Available online 15 October 2010

Keywords:
Hypersonics
Plasma radiation
Nonequilibrium

ABSTRACT

A *k*-distribution model is presented for gas mixtures in thermodynamic nonequilibrium, containing strongly radiating atomic species N and O together with molecular species of N_2, N_2^+, NO and O_2. In the VUV range of the spectrum there is strong absorption of atomic radiation by bands of N_2. For this spectral range, a multi-scale model is presented, where RTEs are solved separately for each emitting species and overlap with other species is treated in an approximate way. Methodology for splitting the gas mixture into scales and evaluation of the overlap parameter between different scales is presented. The accuracy of the new model is demonstrated by solving the radiative transfer equation along the stagnation line flow field of the Crew Exploration Vehicle (CEV).

1. Introduction

Radiation from the shock layer during atmospheric entry plays a significant role in the design of modern space vehicles. Efficient and accurate modeling of shock layer radiation is absolutely necessary for the optimum design of new generation space vehicles. Recently, a number of radiative heat transfer studies have been made, primarily in the context of the Stardust [1] and the Crew Exploration Vehicles [2], emphasizing the need for accurate predictions of radiative heat loads.

NEQAIR96 [3] has been the most widely used code to perform nonequilibrium radiative calculations. NEQAIR96 provides line-by-line data of nonequilibrium radiative properties of hypersonic shock layer plasmas, along with a primitive one-dimensional radiative transport algorithm. The strong spectral structure of radiative emission requires a line-by-line (LBL) solution of the RTE at several hundred thousand wavelengths, making it extremely expensive and unfeasible for solving radiation problems coupled with a flow solver. An accurate and efficient radiation model must include sophisticated spectral modelling, and must maintain nearly line-by-line accuracy, while also minimizing the number of RTE evaluations.

It has been shown in the field of atmospheric radiation that, for a small spectral interval in a homogeneous medium, the absorption coefficient may be reordered into a monotonic *k*-distribution, which yields exact results at a small fraction of the time required for line-by-line calculations [4,5]. More recently, such *k*-distribution methods have been applied to the full spectrum and to inhomogeneous media [6,7]. Over the years a number of new adaptations of the *k*-distribution method has evolved. The problem of inhomogeneity is addressed by using one of the two different approaches: the scaling approximation or the assumption of a correlated *k*-distribution [7]. Both the scaled and correlated-*k* approaches may result in significant errors when dealing with inhomogeneous media, because neither the scaled nor the correlated assumptions are ever truly accurate. The resulting errors and the applicability of scaled and correlated-*k* method have been discussed by Modest [7]. It was recognized

* Corresponding author at: University of California, Merced, CA 95343, United States. Tel.: +1 209 228 4113.
E-mail addresses: azb162@psu.edu (A. Bansal), MModest@eng.ucmerced.edu (M.F. Modest), dalevin@psu.edu (D.A. Levin).

0022-4073/$ - see front matter © 2010 Elsevier Ltd. All rights reserved.
doi:10.1016/j.jqsrt.2010.09.012

Nomenclature

a	nongray stretching function of k-distributions, dimensionless
f	k-distribution, cm
g	cumulative k-distribution
I	intensity, W/cm^2 sr
$I_{b\lambda}$	Planck function, W/cm^2 Å sr
k,k^*	reordered absorption coefficient, cm^{-1}
M	total number of emission scales
n,$\underline{n}$	number density (vector), cm^{-3}
N	total number of narrow bands
Greek	
λ	overlap parameter, cm^{-1}
$\underline{\phi}$	gas state vector

[8–10] that, in high-temperature combustion applications, at significantly different temperatures different spectral lines dominate the radiative transfer, and the assumption of a correlated absorption coefficient breaks down. Similarly, in a mixture of gases the correlation breaks down in the presence of strong concentration gradients, as recognized by Modest and Zhang [6]. To overcome some of these difficulties, Modest and Zhang developed the multi-scale full-spectrum correlated-k distribution method MSFSCK [11], in which different lines are placed into separate "scales" based on their temperature dependence. The MSFSCK method is similar to the fictitious-gas-based ADF method [12], where for M number of fictitious gases or spectral groups M^2 RTEs are solved. In contrast, the MSFSCK method avoids the extra computational cost problem by introducing an approximate overlap parameter, and requires only M RTE solutions. The approximate treatment of overlap between different scales may lead to slightly poor accuracy in the MSFSCK method.

In typical Earth reentry conditions, high-temperature gases in the shock layer are highly dissociated, and the predominant contributions to radiation come from the two atomic species N and O [13]. In the field of atomic line radiation the reordering concept was introduced by Hermann and Schade [14] for high-temperature cylindrical nitrogen arcs. More recently, Bansal et al. [15,16] have developed a multi-group FSCK method for radiative transfer in hypersonic nonequilibrium flows, containing the strongly radiating atomic species of N and O. Bansal et al. have discussed various challenges posed by extreme temperature and concentration gradients and nonequilibrium distribution of population of various energy modes. They also developed a database of narrow-band k-distributions, from which any desired full-spectrum k-distribution can be calculated on-the-fly, which resulted in great reduction of the computational time [16].

In the development of their FSCK method, Bansal et al. neglected the overlap between N and O species, which was found to be a valid assumption [15,16]. It will be shown in this paper that the molecular radiation in visible and infrared part of the spectrum is optically thin, and the overlap between atomic and molecular species can be neglected. In contrast, overlap between atomic radiation and molecular bands is important in the VUV part of the spectrum. For such cases k-distributions for gas mixtures need to be developed. However, it is not straightforward to apply the FSK method to gas mixtures. It requires to combine the individual k-distributions into a single k-distribution. As k-distributions do not retain any information of spectral location of absorption lines in various band systems, it is impossible to combine the individual k-distributions exactly. Solovjov and Webb [17] have proposed a number of approximate mixing models for k-distributions, such as convolution, superposition, multiplication and hybrid models. These models rely on the observation that the absorption coefficients from different species are statistically uncorrelated. Taine and Soufiani [18] have shown that very accurate values of transmissivities of gas mixtures can be obtained by multiplying transmissivities of individual gas species, provided the absorption coefficient of different species are statistically uncorrelated. Based on this observation, Modest et al. [19] have developed a narrow-band-based mixing model for k-distributions. Modest et al. have demonstrated that their mixing model yields much more accurate results than the multiplication model of Denison and Webb. Although all these mixing models do provide a methodology to obtain k-distributions for gas mixtures, their application to strongly nonhomogeneous media may result in significant errors. Also, all these mixing models were developed for thermodynamic equilibrium, and they cannot be directly applied to the nonequilibrium case. Lamet et al. [20] have developed a statistical narrow-band (SNB) model for applications to the nonequilibrium plasmas; however, the model was applied to mixtures containing molecular species only, and gas mixtures containing atomic as well as molecular species with strong spectral overlap were not treated.

The work here is an improvement over our earlier work, where a multi-scale k-distribution model was presented for gas mixtures containing strongly radiating atomic species together with the molecular species of N_2, N_2^+, NO, O_2 [13]. The model takes into account the strong spectral overlap between the atomic radiation and molecular bands in the VUV region and exploits the optically thin nature of molecular radiation elsewhere in the spectrum. The main goal of the present work is to develop an efficient k-distribution method for mixtures containing atomic species (N and O), and bands of N_2 in the VUV. Here an improved model for overlap between scales will be presented, with efficient evaluation of overlap factors from a narrow-band k-distribution database [16] (as opposed to from line-by-line absorption coefficient data employed in the earlier work).

2. Radiative transfer in hypersonic reentry flows

Radiation in hypersonic flows is marked by the strong atomic lines in VUV and infrared and a large number of optically thin molecular band systems in visible and infrared. Total molecular emission may be less than 1%

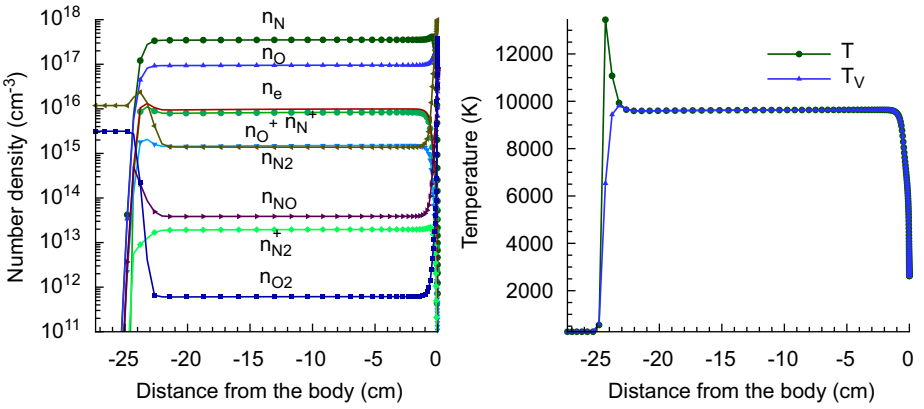

Fig. 1. CEV stagnation line flow-field at peak heating.

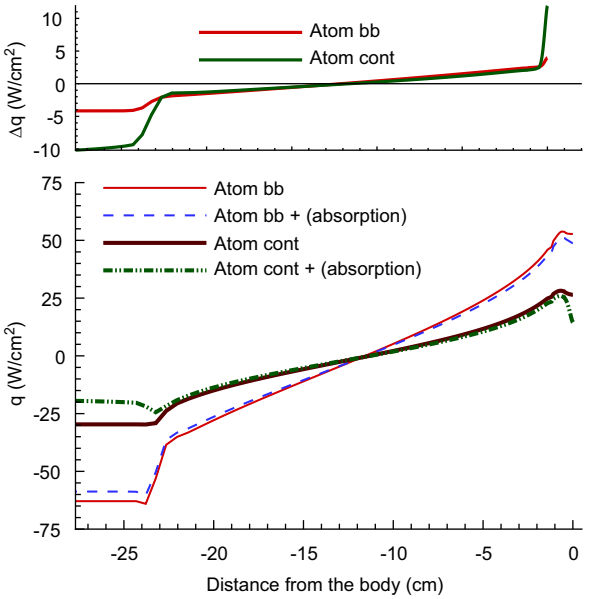

Fig. 2. Absorption of atomic radiation by molecular bands of N_2.

of the total emission [13]. However, due to optically thin nature, unlike atomic radiation, most of it escapes from the shock layer. Thus, molecules also have a significant effect on overall wall heat fluxes. N_2^+ and NO are the most important molecular species from a wall heat flux point of view.

A part from optically thin bands in visible and infrared, some bands of N_2 in VUV are optically very thick, and absorb a significant amount of radiation emitted by atomic species [13]. To demonstrate the effect of absorption in the boundary layer of a spacecraft, heat fluxes were calculated for the crew exploration vehicle (CEV), the stagnation line flow field obtained from a 2D run of the DPLR code [21] at 53 km altitude and Mach 29 conditions is shown in Fig. 1. The line-by-line heat flux results shown in Fig. 2 demonstrate the effect of absorption by N_2 on atomic radiation in the spectral range < 1750 Å. Two different sets of results are plotted, one for emission from only atomic bound–bound lines and the other for emission from atomic continuum, each indicating a significant reduction in wall heat flux due to absorption in the boundary layer. For this flow field the effect of absorption is more pronounced for atomic continuum than atomic bound–bound. It was also observed that the VUV bands of N_2 do not contribute to the heat flux. In NEQAIR as well as in Johnston's radiation model [22,23], the population of upper electronic states of N_2 is calculated by assuming those states in dissociative equilibrium with the atoms, which results in very little emission from these bands.

3. Multi-scale full-spectrum *k*-distribution

When solving an RTE with a *k*-distribution model the absorption coefficients are assumed to be correlated, but this assumption of a correlated absorption coefficient may not be valid for the entire gas mixture; however, one can split the gas or gas mixture into components (scales), such that absorption coefficients within each scale are correlated [11]. This scaling may be done by separating species and/or according to lower level energies of absorption lines for a single species. Following the work of Zhang and Modest [11], the gas mixture is split into M different scales. The total absorption coefficient for the gas mixture can be written as

$$\kappa_\lambda(\underline{\phi}) = \sum_{m=1}^{M} \kappa_{m\lambda}(\underline{\phi}) \tag{1}$$

where $\underline{\phi}$ is the gas state vector which, in general, includes number densities of different species and four temperatures T, T_e, T_V and T_R. Summation in Eq. (1) is taken over all scales. The RTE for the nonequilibrium gas mixture can be written similar to the equilibrium case as [24]

$$\frac{dI_\lambda}{ds} = \sum_{m=1}^{M} \kappa_{m\lambda}(\underline{\phi}) I^{ne}_{bm\lambda}(\underline{\phi}) - \left(\sum_{m=1}^{M} \kappa_{m\lambda}(\underline{\phi}) \right) I_\lambda \tag{2}$$

where $I^{ne}_{bm\lambda}$ is the nonequilibrium Planck function and $\kappa_{m\lambda}(\underline{\phi})$ is the absorption coefficient for scale m. Unlike in thermodynamic equilibrium, the Planck function in nonequilibrium is defined separately for each gas species or

scale as

$$I^{ne}_{bm\lambda} = \frac{\varepsilon_{m\lambda}(\underline{\phi})}{\kappa_{m\lambda}(\underline{\phi})} \tag{3}$$

This makes the multi-scale full-spectrum k-distribution model ideally suited for gas mixtures in nonequilibrium plasmas. When dealing with a mixture of atoms and molecules, atoms may form one scale and molecular bands another scale. Molecular bands can further be split into different scales, considering each band as a separate scale. Now, splitting the total spectral intensity into M terms, one for each scale, i.e.,

$$I_\lambda = \sum_{m=1}^{M} I_{m\lambda} \tag{4}$$

substituting Eq. (4) into Eq. (2) and separating the equation for the m-th scale,

$$\frac{dI_{m\lambda}}{ds} = \kappa_{m\lambda}(\underline{\phi}) I^{ne}_{bm\lambda}(\underline{\phi}) - \left(\sum_{n=1}^{M} \kappa_{n\lambda}(\underline{\phi})\right) I_{m\lambda}, \quad m = 1,2 \ldots M \tag{5}$$

Each of these M equations is an RTE for the spectral intensity emitted by one gas scale, but attenuated by the entire gas mixture. Next, Eq. (5) is reordered by multiplying with $\delta(k_m - \kappa_{m\lambda}(\underline{\phi}_0))$ and integrating over the entire spectrum. Here $\kappa_{m\lambda}(\underline{\phi}_0)$ is the absorption coefficient of the m-th scale evaluated at some reference state $\underline{\phi}_0$. This leads to

$$\frac{dI_{mk}}{ds} = k^*_m(\underline{\phi},k_m) I^{ne}_{bm}(\underline{\phi}) f_m(\underline{\phi},\underline{\phi}_0,k_m) - \int_0^\infty \left(\sum_{n=1}^{M} \kappa_{n\lambda}(\underline{\phi})\right) \delta(k_m - \kappa_{m\lambda}(\underline{\phi}_0)) I_{m\lambda}\, d\lambda \tag{6}$$

provided that at every wavelength across the entire spectrum, where $\kappa_{m\lambda}(\underline{\phi}_0) = k_m$, we also have a unique value for $\kappa_{m\lambda}(\underline{\phi}) = k^*_m(\underline{\phi},k)$ everywhere within the medium. Here I_{mk} and f_m are defined as

$$I_{mk} = \int_0^\infty I_{m\lambda} \delta(k_m - \kappa_{m\lambda}(\underline{\phi}_0))\, d\lambda \tag{7}$$

$$f_m(\underline{\phi},\underline{\phi}_0,k_m) = \frac{1}{I^{ne}_{bm}(\underline{\phi})} \int_0^\infty I^{ne}_{bm\lambda}(\underline{\phi}) \delta(k_m - \kappa_{m\lambda}(\underline{\phi}_0))\, d\lambda \tag{8}$$

where $f_m(\underline{\phi},\underline{\phi}_0,k)$ is the Planck function weighted full-spectrum k-distribution for scale m, which depends on reference state conditions $\underline{\phi}_0$ through the absorption coefficient and local conditions $\underline{\phi}$ through the nonequilibrium Planck function. Now the above equation can be rewritten as

$$\frac{dI_{mk}}{ds} = k^*_m(\underline{\phi},k_m) I^{ne}_{bm}(\underline{\phi}) f_m(\underline{\phi},\underline{\phi}_0,k_m) - \lambda_m(\underline{\phi},k_m) I_{mk} \tag{9}$$

where λ_m is defined as the overlap factor of the m-th scale with the entire gas. In general,

$$\lambda_m I_{mk} = \int_0^\infty \sum_{n=1}^{M} \kappa_{n\lambda}(\underline{\phi}) \delta(k_m - \kappa_{m\lambda}(\underline{\phi}_0)) I_{m\lambda}\, d\lambda = \sum_{n=1}^{M} \int_0^\infty \kappa_{n\lambda} \delta(k_m - \kappa_{m\lambda}(\underline{\phi}_0)) I_{m\lambda}\, d\lambda = I_{mk} \sum_{n=1}^{M} \lambda_{nm} \tag{10}$$

Here λ_{nm} is the spectral overlap of scale m with scale n. Note that $\lambda_{mm} = k_m$ and $I_{m\lambda} = 0$ wherever $\kappa_{m\lambda} = 0$, as $I_{m\lambda}$ is related to emission from the m-th scale. Also, if there is no overlap, $\lambda_m = k_m$.

Now dividing Eq. (9) by the k-distribution at the reference state $f_m(\underline{\phi}_0,\underline{\phi}_0,k_m)$, the RTE is transformed into the much smoother g-space

$$\frac{dI_{mg}}{ds} = k^*_m(\underline{\phi}_0,\underline{\phi},g_m) I^{ne}_{bm}(\underline{\phi}) a_m(\underline{\phi},\underline{\phi}_0,g_m) - \lambda_m(\underline{\phi}_0,\underline{\phi},g_m) I_{mg} \tag{11}$$

with

$$I_{mg} = I_{mk}/f_m(\underline{\phi}_0,\underline{\phi}_0,k_m) = \int_0^\infty I_{m\lambda} \delta(k_m - \kappa_{m\lambda}(\underline{\phi}_0))\, d\lambda / f_m(\underline{\phi}_0,\underline{\phi}_0,k_m) \tag{12}$$

where g_m is the cumulative k-distribution and $a_m(\underline{\phi},\underline{\phi}_0,g_m)$ is a weight or nongray stretching function given by

$$g_m(\underline{\phi}_0,\underline{\phi}_0,k_m) = \int_{k_m}^{k_{m,max}} f_m(\underline{\phi}_0,\underline{\phi}_0,k_m)\, dk_m \tag{13}$$

$$a_m(\underline{\phi},\underline{\phi}_0,g_m) = \frac{f_m(\underline{\phi},\underline{\phi}_0,k_m)}{f_m(\underline{\phi}_0,\underline{\phi}_0,k_m)} = \frac{dg_m(\underline{\phi},\underline{\phi}_0,k_m)}{dg_m(\underline{\phi}_0,\underline{\phi}_0,k_m)} \tag{14}$$

where, for numerical precision reasons, a monotonically *decreasing* cumulative k-distribution has been defined [15]. In numerical calculations it is difficult to evaluate the ratio of the k-distributions f_m, due to their erratic behavior (having singularities at each minimum and maximum of the absorption coefficient [7]); it is much more convenient to evaluate the smoothened derivative dg_m/dk_m, as indicated in Eq. (14).

3.1. Evaluation of overlap factor

The overlap factor in Eq. (11) is evaluated in an approximate way, such that the multi-scale FSCK model obtains the exact result for emitted intensity emanating from a homogeneous layer [11]. First, Eq. (11) is integrated over a homogeneous slab of thickness X. For a homogeneous slab the weight function $a_m = 1$ and $k^*_m(\underline{\phi}_0,\underline{\phi},g_m) = k_m(\underline{\phi},g_m)$. This gives

$$I_{mg} = \frac{k_m(\underline{\phi},g_m) I^{ne}_{bm}(\underline{\phi})}{\lambda_m(\underline{\phi},g_m)} (1 - e^{-\lambda_m(\underline{\phi},g_m)X}) \tag{15}$$

The total intensity for the m-th scale can then be determined from

$$I_m = \int_0^1 \frac{k_m(\underline{\phi},g_m) I^{ne}_{bm}(\underline{\phi})}{\lambda_m(\underline{\phi},g_m)} (1 - e^{-\lambda_m(\underline{\phi},g_m)X})\, dg_m = \int_0^\infty \frac{k_m f_m(\underline{\phi},k_m) I^{ne}_{bm}(\underline{\phi})}{\lambda_m(\underline{\phi},k_m)} (1 - e^{-\lambda_m(\underline{\phi},k_m)X})\, dk_m \tag{16}$$

Eq. (5) can also be reordered by multiplying with $\delta(k - \kappa_\lambda(\underline{\phi}))$, i.e., the total absorption coefficient. For a homogeneous cell

this gives

$$\frac{dI_{mk}}{ds} = \overline{k}_m(\underline{\phi},k)I^{ne}_{bm}(\underline{\phi}) - kI_{mk} \tag{17}$$

where

$$\overline{k}_m(\underline{\phi},k) = \frac{1}{I^{ne}_{bm}(\underline{\phi})}\int_0^\infty \kappa_{m\lambda}(\underline{\phi})I^{ne}_{bm\lambda}(\underline{\phi})\delta(k-\kappa_\lambda)\,d\lambda \tag{18}$$

Integrating Eq. (17) leads to

$$I_{mk} = \frac{\overline{k}_m(\underline{\phi},k)I^{ne}_{bm}(\underline{\phi})}{k}\left(1-e^{-k(\underline{\phi})X}\right) \tag{19}$$

The total intensity is obtained by integrating over k-space as

$$I_m = \int_0^\infty \frac{\overline{k}_m(\underline{\phi},k)I^{ne}_{mb}(\underline{\phi})}{k}(1-e^{-k(\underline{\phi})X})\,dk \tag{20}$$

which is exact for the homogeneous case. The total intensity obtained by the two methods for a homogeneous layer from Eqs. (16) and (20) must be the same. Comparing the results leads to the following two requirements:

$$\lambda_m(\underline{\phi},k_m) = k(\underline{\phi}) \tag{21}$$

and

$$k_m(\underline{\phi})f_m(\underline{\phi},k_m)\,dk_m = \overline{k}_m(\underline{\phi},k)\,dk \tag{22}$$

A computationally convenient way to solve the above, as suggested by Zhang and Modest [11], is

$$\int_0^{k_m} k_m(\underline{\phi})f_m(\underline{\phi},k_m)\,dk_m = \int_0^{k=\lambda_m} \overline{k}_m(\underline{\phi},k)\,dk \tag{23}$$

This is an implicit relation from which λ_m-values need to be evaluated for a set of k_m-values. In practice, the overlap factor must be evaluated for all gas states, and will be a function of all number densities and temperatures. It is very costly to evaluate the overlap factor on-the-fly for all gas states; however, it cannot be databased effectively as it depends on a large number of parameters. Fortunately, narrow-band k-distribution databases can greatly simplify the evaluation of overlap parameters [25]. Evaluation of the overlap parameter from narrow-band k-distribution databases will be discussed in Section 4.

3.2. Application of multi-scale model to heat transfer calculations

In this section an outline of the application of the multi-scale k-distribution model to gas mixtures is given. First, the spectrum is broken into two parts: the VUV and UV occupy the short wavelength part of the spectrum, separated from the visible and infrared. Next, each part-spectrum is broken into three scales: the first scale comprises bound–bound atomic lines, the second scale the atomic continuum and the third scale all molecular bands of interest.

In the VUV and UV (spectrum below <1750 Å), for bound–bound radiation (Scale 1), Eq. (23) is first solved for the overlap factor using about 5000 points. Absorption from the entire gas, i.e., atomic lines, atomic continuum and molecular bands of N_2 is considered. The overlap factor for two typical gas states taken from the CEV flow field is plotted in Fig. 3. Gas properties for these two states are given in Table 1. λ_m is the sum of k_m and the contribution from overlap with all other species, implying $\lambda_m \geq k_m$ always. State 1 is taken from the colder boundary layer region, where the concentration of molecular N_2 is very large. For this state, there is significant overlap between the scales. State 2 is taken from the hotter regions of the flow field, where concentration of N_2 is small, and the overlap is relatively minor. As overlap occurs mostly in line wings, it is more significant at smaller k-values. The overlap factor is then interpolated to a smaller number of points chosen according to Gaussian quadrature schemes to reduce the number of RTE evaluations. In this unoptimized work, 128 RTEs are solved to ensure accuracy.

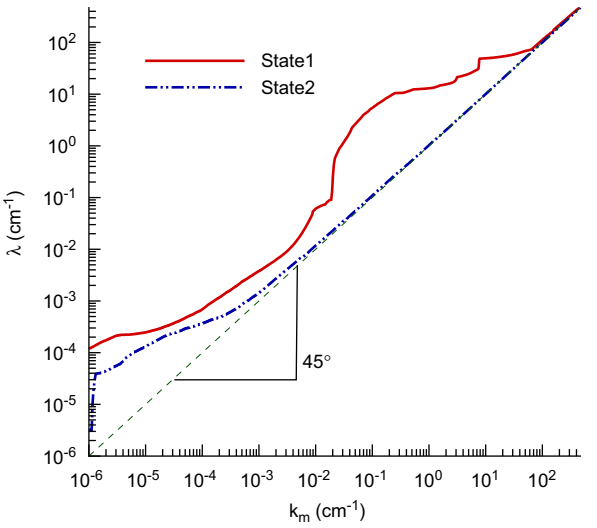

Fig. 3. Overlap factor for Scale 1 as a function reordered absorption coefficient: (a) Cell 1, (b) Cell 2.

Table 1
Flow conditions for two cell problem.

	Cell 1	Cell 2
$T=T_e=T_V=T_R$ (K)	3850	9628
n_e (cm^{-3})	4.2×10^{12}	9.8×10^{15}
n_N (cm^{-3})	6.5×10^{14}	3.5×10^{17}
n_O (cm^{-3})	2.0×10^{17}	9.5×10^{16}
n_{N^+} (cm^{-3})	7.0×10^{7}	8.3×10^{15}
n_{O^+} (cm^{-3})	4.0×10^{11}	1.5×10^{15}
n_{N_2} (cm^{-3})	8.2×10^{17}	1.4×10^{15}

The overlap factor approach can be applied to atomic continuum radiation (Scale 2) as well; however, the nature of atomic continuum radiation is very different from atomic bound–bound lines. The continuum k-distribution has many distinct steps, which cannot be integrated using a standard integration procedure, such as the Gaussian quadrature used for bound–bound k-distributions. Due to this fact, Scale 2 is treated slightly different from Scale 1, as discussed in the next section.

Finally, the third scale comprises the three molecular bands of N_2 present in the VUV/UV; however, there is no significant emission from molecular bands of N_2 in the VUV and, therefore, no RTE needs to be solved for this scale. Thus, effectively, RTEs for only two scales are solved.

As already mentioned, molecular radiation in the visible and infrared is optically thin. Gray calculations for these molecular bands provide very accurate results compared to the expensive LBL method [26]. Also, these bands do not absorb any significant radiation from atomic lines; therefore, they can be treated independently of atomic lines. For this region, Scale 1 is treated using the standard FSCK model (32 quadrature points), while the gray approximation is made for Scales 2 and 3, requiring a total of 34 RTE evaluations. The overlap between scales can be neglected without incurring any significant error.

3.3. Mixing model for Scale 2: emission from atomic continuum radiation

Continuum radiation from N and O is marked by many distinct steps in the absorption coefficient. Over a narrow-band the absorption coefficient does not change very significantly and, thus, over each narrow-band the absorption coefficient can be approximated by a constant number [16]. There are about 16 steps in the continuum spectrum for which mixing model needs to be developed to predict the amount of absorption by molecular bands; atomic bound–bound lines are very narrow, and does not significantly absorb the continuum radiation. To account for absorption over each narrow-band, the absorption coefficient of molecular bands needs to be represented correctly in terms of k-distributions. The RTE for this case can be written as

$$\frac{dI_\lambda}{ds} = \kappa_{c\lambda}(\underline{\phi})I_{bc\lambda}(\underline{\phi}) - [\kappa_{c\lambda}(\underline{\phi}) + \kappa_{n\lambda}(\underline{\phi})]I_\lambda \tag{24}$$

where $\kappa_{c\lambda}$ and $I_{bc\lambda}$ are absorption coefficient and Planck function for the continuum, respectively, and $\kappa_{n\lambda}$ is the absorption coefficient of molecular bands. Applying the reordering scheme to the above equation by multiplying with $\delta(k-\kappa_{n\lambda}(\underline{\phi}_0))$, and integrating over the i-th narrow-band, leads to

$$\frac{dI_{ik}}{ds} = \kappa_{ci}(\underline{\phi})I_{bci}(\underline{\phi})f_i(\underline{\phi}_0,k) - (c_i(\underline{\phi}) + k_i^*(\underline{\phi},k))I_{ik}$$

provided that at every wavelength across the entire spectrum, where $\kappa_{n\lambda}(\underline{\phi}_0) = k$, we also have a unique value for $\kappa_{n\lambda}(\underline{\phi}) = k^*(\underline{\phi},k)$ everywhere within the medium. Here, $\kappa_{ci}(\underline{\phi})$ and $I_{bci}(\underline{\phi})$ are absorption coefficient and narrow-band integrated Planck function for the continuum, taken as constants over a narrow-band. In Eq. (25) I_{ik} and f_i are defined as

$$I_{ik} = \int_{\Delta\lambda_i} I_\lambda \delta(k-\kappa_{n\lambda}(\underline{\phi}_0))\, d\lambda \tag{25}$$

$$f_i(\underline{\phi}_0,k_m) = \frac{1}{\Delta\lambda_i}\int_{\Delta\lambda_i} \delta(k-\kappa_{n\lambda}(\underline{\phi}_0))\, d\lambda \tag{26}$$

where $f_i(\underline{\phi}_0,k)$ is the k-distribution for molecules for the i-th narrow-band. Dividing the above equation by the k-distribution $f_i(\underline{\phi}_0,k)$ leads to

$$\frac{dI_{ig}}{ds} = \kappa_{ci}(\underline{\phi})I_{bci}(\underline{\phi}) - (\kappa_{ci}(\underline{\phi}) + k_i^*(\underline{\phi},g_i))I_{ig} \tag{27}$$

with

$$I_{ig} = I_{ik}/f_i(\underline{\phi}_0,k_m) = \int_{\Delta\lambda} I_\lambda \delta(k-\kappa_{n\lambda}(\underline{\phi}_0))\, d\lambda / f_i(\underline{\phi}_0,k) \tag{28}$$

$$g_i(\underline{\phi}_0,k) = \int_k^{k_{max}} f_i(\underline{\phi}_0,k)\, dk \tag{29}$$

Eq. (27) is the reordered RTE in g-space for emission from atomic continuum only but absorption by the entire gas. To integrate the RTE in g-space, four quadrature points are used for each narrow-band, thus requiring $16 \times 4 = 64$ RTE evaluations in total.

4. Evaluation of overlap parameter using k-distribution database

In the multi-scale model for gas mixtures the overlap parameter between different scales is evaluated from high resolution data of absorption coefficients. The difficulty and computational effort required to achieve this make it impractical for use in heat transfer calculations. For IR radiation in combustion applications Wang and Modest [25] developed a scheme, which allows very fast evaluation of the overlap parameter. That scheme is based on two important observations: (1) full-spectrum k-distributions can be assembled very efficiently from narrow-band k-distribution databases, (2) absorption coefficients of different species are statistically uncorrelated. The statistical independence of absorption coefficients allows to write the transmissivity of gas mixtures in terms of component transmissivities. However, the same argument of statistical independence cannot be made for atomic bound–bound lines mixed with the erratically varying molecular spectrum of N_2. In contrast, here it will be assumed, for the purpose of evaluating the overlap factor, that absorption coefficients of overlapping species (molecular N_2 and atomic continuum) can be approximated with their averages over the narrow-band. To develop the method, Eq. (18) is substituted into the RHS of Eq. (23),

$$RHS = \int_0^{k=\lambda_m} \frac{1}{I_{bm}^{ne}} \int_0^\infty \kappa_{m\lambda} I_{bm\lambda}^{ne} \delta(k-\kappa_\lambda)\, d\lambda\, dk$$

Now, dividing the full spectrum into N narrow bands

$$RHS = \int_0^{k=\lambda_m} \sum_{i=1}^{N} \frac{I_{bmi}^{ne}}{I_{bm}^{ne}} \frac{1}{I_{bmi}^{ne}} \int_{\Delta\lambda_i} \kappa_{m\lambda} I_{bm\lambda}^{ne} \delta(k-\kappa_\lambda)\, d\lambda\, dk$$
$$= \sum_{i=1}^{N} \frac{I_{bmi}^{ne}}{I_{bm}^{ne}} \int_0^{k=\lambda_m} \overline{k}_{m,i}(\underline{\phi},k)\, dk \tag{30}$$

where $\overline{k}_{m,i}(\underline{\phi},k)$ is the narrow-band equivalent to $\overline{k}_m(\underline{\phi},k)$ and I_{bmi}^{ne} is the narrow-band integrated Planck function, defined as

$$I_{bmi}^{ne} = \int_{\Delta\lambda_i} I_{bm\lambda}^{ne}\, dk \tag{31}$$

The problem is thus reduced to the evaluation of $\int_0^{k=\lambda_m} \overline{k}_{m,i}(\underline{\phi},k)\, dk$ in terms of narrow-band k-distributions.

At this stage the absorption coefficients of atomic continuum and molecular bands of N_2 are replaced by appropriate averages, and are represented as $\overline{\kappa}_i$ for the i-th narrow-band. Then the integral in Eq. (30) can be

written as

$$\int_0^{k=\lambda_m} \frac{1}{I^{ne}_{bmi}} \int_{\Delta\lambda_i} \kappa_{m\lambda} I^{ne}_{bm\lambda} \delta(k-\kappa_\lambda)\, d\lambda\, dk = \int_0^{k_m=\lambda_m-\overline{\kappa}_i} \frac{1}{I^{ne}_{bmi}} \int_{\Delta\lambda_i} \kappa_{m\lambda} I^{ne}_{bm\lambda} \delta(k_m-\kappa_{m\lambda})\, d\lambda\, dk_m = \int_0^{k_m=\lambda_m-\overline{\kappa}_i} k_m f_{m,i}(k_m) dk_m = \int_1^{g_{m,i}(k_m=\lambda_m-\overline{\kappa}_i)} k_m\, dg_{m,i} \tag{32}$$

Thus, the RHS can be written as

$$RHS = \sum_{i=1}^{N} \frac{I^{ne}_{bmi}}{I^{ne}_{bm}} \int_1^{g_{m,i}(k_m=\lambda_m-\overline{\kappa}_i)} k_m\, dg_{m,i} \tag{33}$$

Similarly, the LHS of Eq. (23) can be written as

$$LHS = \int_0^{k_m} k_m(\underline{\phi}) \frac{1}{I^{ne}_{bm}} \int_0^{\infty} I^{ne}_{bm\lambda} \delta(k-\kappa_{m\lambda})\, d\lambda\, dk_m = \sum_{i=1}^{N} \frac{I^{ne}_{bmi}}{I^{ne}_{bm}} \int_1^{g_{m,i}(k_m)} k_m(\underline{\phi})\, dg_{m,i} \tag{34}$$

Equating the LHS and RHS, we obtain the following expression for the determination of the overlap factor:

$$\sum_{i=1}^{N} \frac{I^{ne}_{bmi}}{I^{ne}_{bm}} \int_1^{g_{m,i}(k_m)} k_m(\underline{\phi})\, dg_{m,i} = \sum_{i=1}^{N} \frac{I^{ne}_{bmi}}{I^{ne}_{bm}} \int_1^{g_{m,i}(k_m=\lambda_m-\overline{\kappa}_i)} k_m\, dg_{m,i} \tag{35}$$

This is an implicit relation from which the λ_m (overlap parameter for species m with the entire gas) need to be evaluated for a set of k_m-values for all gas states.

Similar to the database of atomic continuum [16], a database of narrow-band-averaged absorption coefficient of N_2 bands was generated. This database along with the k-distribution and atomic continuum databases provide a very efficient method to predict the effect of N_2 absorption on atomic radiation. Because in the k-distribution database data are assembled for fixed Gaussian quadrature points, evaluation of the integrals in Eq. (35) is very efficient [16,25]. It will be shown that the use of narrow-band-averaged absorption coefficient has no significant effect on overall solution accuracy.

5. Sample calculations

5.1. Two cell problem

The accuracy of the new model is demonstrated by solving a simple two-cell problem containing a mixture of gases with strong temperature and concentration gradients. More severe inhomogeneous conditions of temperatures and gas concentrations are taken than actually present in typical hypersonic shock layers. Cell 2 is assumed to be of constant thickness of 1 cm, while Cell 1 has a variable thickness. Both cells are bounded by cold black walls. An example of the conditions in the two cells is given in Table 1. These conditions have been appropriately chosen from actual shock layer conditions. Such two-cell problems with typical conditions serve as an acid test for the method because of their abrupt step-changes in conditions. In actual applications gradients are much more benign and the accuracy of the model can be expected to be better. To test the accuracy of the new overlap model only the VUV/UV part of the spectrum is considered.

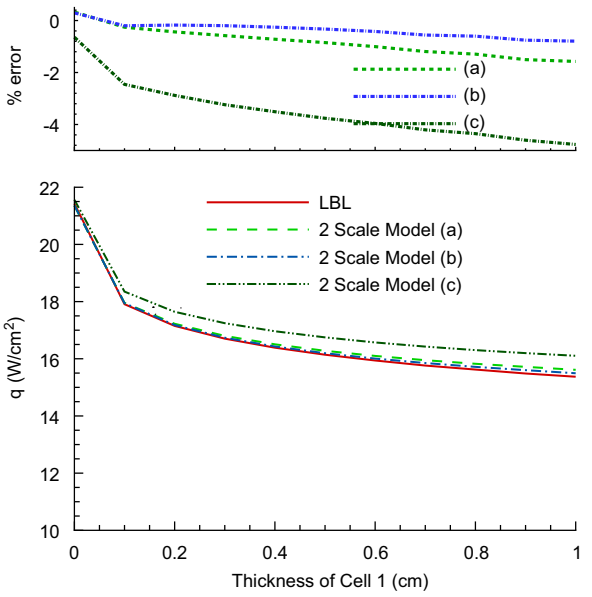

Fig. 4. Heat flux exiting the cold cell with varying Cell 1 thickness: (a) line-by-line absorption coefficient, (b) narrow-band-averaged absorption coefficient of absorbing scales and (c) no overlap for Scale 1.

A comparison of heat flux exiting the cold cell is given in Fig. 4. Results marked as (a) use line-by-line absorption coefficient data for N_2 bands and atomic continuum for the calculation of the overlap parameter for Scale 1 (of Section 3.2), while results marked as (b) use narrow-band-averaged absorption coefficients. It was shown by Bansal et al. [15] that the full-spectrum k-distribution model may lead to significant errors when applied to severely nonhomogeneous problems, even in the absence of absorption by other scales. Therefore, to compare the accuracy of the multi-scale model it is necessary that the k-distribution model predicts accurate results in the absence of absorption by other scales. Almost all of the emission comes from Cell 2, which gets absorbed in Cell 1. If the reference state in the problem is set to the gas state in Cell 2, emission from Cell 2 is predicted correctly and, therefore, wall heat flux is predicted correctly in the absence of absorption by other scales.

The maximum error for the 2-scale model was found to be less than 2% at the largest value of Cell 1 thickness. As the thickness of Cell 1 is increased, absorption becomes more and more important. Increase in Cell 1 thickness also increases the importance of overlap between the two species. Since the overlap factor is evaluated in an approximate way, this results in slightly larger error in the heat flux result. It is also observed that approximating the absorption coefficients by narrow-band averages gives slightly different results. This is apparently due to error cancellation between the approximate overlap factor and averaged absorption coefficients. However, the difference between the two results is not significant and, therefore, the absorption coefficients can be replaced by narrow-band-averaged quantities. Fig. 2 also shows that the effect of N_2 absorption is stronger on the atomic continuum,

which is modeled exactly by solving the RTE on a narrow-band basis. To model the relatively less significant effect of overlap on atomic bound–bound radiation, the approximate approach for the overlap factor using a narrow-band-averaged absorption coefficient is a reasonably good choice, since it provides good accuracy and efficient evaluation of the overlap factor from *k*-distribution databases. However, neglecting the overlap between the atomic bound–bound scale and other scales leads to inaccuracies, as is clear from the relatively larger errors shown in Fig. 4. In the present 2-scale model 128 RTEs were solved for Scale 1, and 64 RTEs for Scale 2, totalling 192 for the entire gas mixture.

5.2. CEV stagnation line flow field

Next, the multi-scale model was applied to the stagnation line flow field of the CEV vehicle. In Fig. 5 the local heat flux and divergence of heat flux for the VUV/UV spectral region, obtained from the multi-scale model, are compared with line-by-line results. The overall agreement between the two results is very good, except very near to the wall. The maximum error in heat flux is about 1.2–1.3%, relative to the wall heat flux value. This small error results from the fact that there is very significant overlap in the near wall region, and therefore, the approximate determination of the overlap factor may not be very accurate. It was also observed that most of this error occurs in solving the RTE for Scale 1, and the solution for Scale 2 is much more accurate. Similarly, for the divergence of the heat flux the agreement is excellent except in the near-wall region. Again, similar accuracy is obtained when absorption coefficients are replaced by narrow-band-averages.

As indicated earlier, the visible/infrared part of the spectrum is effectively treated by neglecting overlap and assuming atomic continuum and molecular radiation to be gray. Heat transfer results obtained with the multi-scale model for this region are compared with line-by-line results in Fig. 6. The excellent agreement between the two results proves the accuracy of the *k*-distribution model for atomic species and the gray assumption for optically thin molecular bands and the atomic continuum. It also proves that the overlap between scales has no significant impact on the radiative flux.

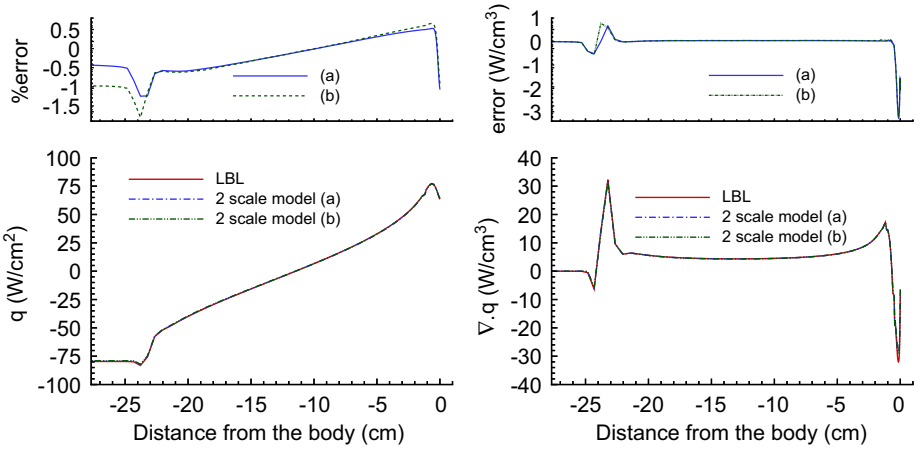

Fig. 5. Results for three scale model in VUV and UV region; heat flux (left) and divergence of heat flux (right).

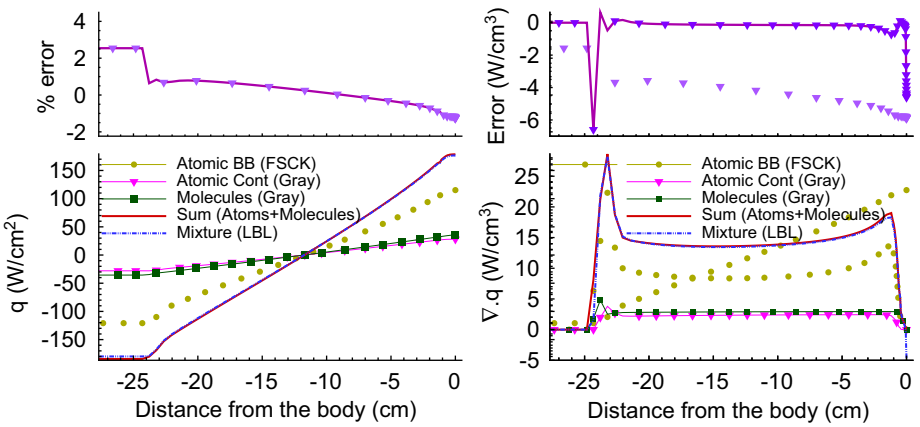

Fig. 6. Results for three scale model in visible and infrared region; heat flux (left) and divergence of heat flux (right).

6. Conclusions

A multi-scale *k*-distribution model was developed for gas mixtures in thermodynamic nonequilibrium. In the VUV region, bands of N_2 were found to strongly absorb radiation from atomic species. For this spectral range, a multi-scale model was presented—RTEs were solved separately for each emitting scale and overlap between scales was treated using an approximate overlap factor. A method for the efficient determination of the overlap factor from narrow-band *k*-distribution database was presented, in which line-by-line absorption coefficients of absorbing scales were replaced by narrow-band-averaged absorption coefficients. For emission from the atomic continuum a method was developed to solve the RTE on a narrow-band basis, modeling the overlap with molecular bands exactly. The narrow-band approach allowed resolving of steps in the absorption spectrum of the continuum. In the visible and infrared region it was found that overlap between different scales is not important due to the optically thin nature of molecular bands there. For this spectral range a gray model was applied to molecular bands and atomic continuum, and the FSCK method was used to treat atomic bound–bound lines. Heat transfer results for a 2 cell problem and the stagnation line flow field of the CEV vehicle show that the new model provides very accurate heat transfer results for gas mixtures at a small fraction of the cost of line-by-line results.

Acknowledgement

The research performed at the Pennsylvania State University was supported by NASA through Grant no. NNX07AC47A.

References

[1] Olynick D, Chen Y-K, Tauber ME. Aerothermodynamics of the stardust sample return capsule. Journal of Spacecraft and Rockets 1999;36(3):442–62.
[2] Bose D, McCorkle E, Thompson E, Bogdanoff D, Prabhu DK, Allen GA, et al. Analysis and model validation of shock layer radiation in air. In: AIAA Paper No. 2008-1246, 2008, 46th AIAA Aerospace Sciences Meeting and Exhibit, Reno, NV.
[3] Whiting E, Park C, Liu Y, Arnold J, Paterson J. NEQAIR96, nonequilibrium and equilibrium radiative transport and spectra program: user's manual. NASA/Ames Research Center, Moffett Field, CA, NASA Reference Publication 1389, December 1996.
[4] Lacis AA, Oinas V. A description of the correlated-*k* distribution method for modeling nongray gaseous absorption, thermal emission, and multiple scattering in vertically inhomogeneous atmospheres. Journal of Geophysical Research 1991;96(D5):9027–63.
[5] Goody RM, Yung YL. Atmospheric radiation—theoretical basis. 2nd ed.. New York: Oxford University Press; 1989.
[6] Modest MF, Zhang H. The full-spectrum correlated-*k* distribution for thermal radiation from molecular gas-particulate mixtures. Journal of Heat Transfer 2002;124(1):30–8.
[7] Modest MF. Narrow-band and full-spectrum *k*-distributions for radiative heat transfer—correlated-*k* vs. scaling approximation. Journal of Quantitative Spectroscopy and Radiative Transfer 2003;76(1):69–83.
[8] Rivière P, Soufiani A, Taine J. Correlated-*k* and fictitious gas methods for H_2O near 2.7 μm. Journal of Quantitative Spectroscopy and Radiative Transfer 1992;48(2):187–203.
[9] Rivière P, Soufiani A, Taine J. Correlated-*k* and fictitious gas model for H_2O infrared radiation in the Voigt Regime. Journal of Quantitative Spectroscopy and Radiative Transfer 1995;53(3):335–46.
[10] Rivière P, Scutaru D, Soufiani A, Taine J. A new *c*-*k* data base suitable from 300 to 2500 K for spectrally correlated radiative transfer in CO_2-H_2O transparent gas mixtures. In: Tenth International Heat Transfer Conference. Taylor Francis; 1994. p. 129–34.
[11] Zhang H, Modest MF. A multi-scale full-spectrum correlated-*k* distribution for radiative heat transfer in inhomogeneous gas mixtures. Journal of Quantitative Spectroscopy and Radiative Transfer 2002;73(2–5):349–60.
[12] Pierrot L, Rivière P, Soufiani A, Taine J. A fictitious-gas-based absorption distribution function global model for radiative transfer in hot gases. Journal of Quantitative Spectroscopy and Radiative Transfer 1999;62(5):609–24.
[13] Bansal A, Modest MF, Levin DA. *k*-distributions for gas mixtures in hypersonic nonequilibrium flows. In: AIAA Paper No. 2010-234, 48th AIAA Aerospace Sciences Meeting, 2010.
[14] Hermann W, Schade E. Radiative energy balance in cylindrical nitrogen arcs. Journal of Quantitative Spectroscopy and Radiative Transfer 1971;12(9):1257–82.
[15] Bansal A, Modest MF, Levin DA. Multigroup correlated-*k* distribution method for nonequilibrium atomic radiation. Journal of Thermophysics and Heat Transfer 2010;24(3):638–46.
[16] Bansal A, Modest MF, Levin DA. Narrow-band *k*-distribution database for atomic radiation in hypersonic nonequilibrium flows. Journal of Heat Transfer, submitted for publication.
[17] Solovjov V, Webb BW. SLW modeling of radiative transfer in multicomponent gas mixtures. Journal of Quantitative Spectroscopy and Radiative Transfer 2000;65:655–72.
[18] Taine J, Soufiani A. Gas IR radiative properties: from spectroscopic data to approximate models. In: Advances in heat transfer, vol. 33. New York: Academic Press; 1999. p. 295–414.
[19] Modest MF, Riazzi RJ. Assembly of full-spectrum *k*-distributions from a narrow-band database; effects of mixing gases, gases and nongray absorbing particles, and mixtures with nongray scatterers in nongray enclosures. Journal of Quantitative Spectroscopy and Radiative Transfer 2004;90(2):169–89.
[20] Lamet JM, Rivie're P, Perrin M, Soufiani A. Narrow-band model for nonequilibrium air plasma radiation. Journal of Quantitative Spectroscopy and Radiative Transfer 2010;111:87–104.
[21] Wright M, Candler G, Bose D. Data-parallel line relaxation method for the Navier–Stokes equations. AIAA Journal 1998;36(9):1603–9.
[22] Johnston CO, Hollis BR. Spectrum modeling for air shock-layer radiation at lunar-return conditions. Journal of Spacecraft and Rockets 2008;45:865–78.
[23] Johnston CO, Hollis BR. Non-Boltzmann modeling for air shock-layer radiation at lunar-return conditions. Journal of Spacecraft and Rockets 2008;45:879–90.
[24] Modest MF. Radiative heat transfer. 2nd ed.. New York: Academic Press; 2003.
[25] Wang L, Modest MF. Narrow-band based multiscale fullspectrum *k*-distribution method for radiative transfer in inhomogeneous gas mixtures. Journal of Heat Transfer 2005;127:740–8.
[26] Bansal A, Modest MF, Levin DA. Application of *k*-distribution method to molecular radiation in hypersonic nonequilibrium flows. In: AIAA Paper No. 2009-3922, 41st AIAA Thermophysics Conference, 2009.